Synthesis of indole inhibitors of silent information regulator 1 (SIRT1), and their evaluation as cytotoxic agents

Hanna Laaroussi, Ying Ding, Yuou Teng, Patrick Deschamps, Michel Vidal, Peng Yu, Sylvain Broussy

Synthesis of indole inhibitors of silent information regulator 1 (SIRT1), and their evaluation as cytotoxic agents

Hanna Laaroussi,[a,$] Ying Ding,[b] Teng Yuou,[b] Patrick Deschamps,[a] Michel Vidal,[a,c] Peng Yu,[b] Sylvain Broussy[a]

[a] Université de Paris, CiTCoM, 8038 CNRS, U 1268 INSERM, F-75006 Paris, France

[b] China International Science and Technology, Cooperation Base of Food Nutrition/Safety and Medicinal Chemistry, College of Biotechnology, Tianjin University of Science and Technology, Tianjin, 300457, China

[c] Service biologie du médicament, toxicologie, AP-HP, Hôpital Cochin, F-75014 Paris, France

[$] Present address: Research Group of Organic Chemistry, Departments of Chemistry and Bio-Engineering Sciences, Vrije Universiteit Brussel, Pleinlaan 2, 1050 Brussels, Belgium

Email: sylvain.broussy@u-paris.fr

Keywords. Cancer, indoles, SIRT1 inhibitors, cytotoxicity assays, bioactive conformation

Abstract

A series of achiral indole analogs of the selective sirtuin inhibitor EX-527 (a racemic, substituted 1,2,3,4 tetrahydrocarbazole) was designed to stabilize the bioactive conformation, and synthesized. These new indoles were evaluated against the isolated sirtuin enzymes SIRT1 and SIRT2, and against a panel of nine human cell lines. Structure-activity relationship studies demonstrated the influence of the substituent at position 3 of the indole. The most potent SIRT1 inhibitor **3h**, bearing an isopropyl substituent, was as potent as EX-527, and more selective for SIRT1 over SIRT2. Compound **3g**, bearing a benzyl substituent, inhibited both sirtuins at micromolar concentration and was more cytotoxic than EX-527 on several cancer cell lines.

1. Introduction

Histone deacetylases (HDACs) are enzymes involved in epigenetic regulation, and their inhibition has been successfully employed to develop cancer therapeutics [1]. Sirtuins are NAD^+-dependent enzymes belonging to the class III of HDACs, and they regulate the activity

and fate of a variety of protein substrates, including histones and transcription factors [2]. There are seven known members in the human sirtuin family of enzymes, SIRT1-7. Due to their broad biological activities, they constitute potential therapeutic targets, and several small molecules able to increase or inhibit their activity have been developed [3, 4]. SIRT1 is the deacetylase that has attracted the most attention so far, in particular for the potential treatment of diseases of aging, including cancer and neurodegenerative disorders [5, 6]. One of the most described potent and selective SIRT1 inhibitors is the 1,2,3,4 tetrahydrocarbazole EX-527 (Selisistat) [7, 8]. Following encouraging animal studies [9], this inhibitor was evaluated in a clinical trial to treat Huntington disease (HD) [10]. The efficacy was not found sufficient to encourage further development of this compound in HD, possibly due to the slow onset of the disease and the comparatively short length (2 weeks) of the clinical trial. Interestingly, in a clinical trial with healthy volunteers, EX-527 exhibited a high bioavailability and good tolerability [11].

The role of SIRT1 inhibitors in cancer is complex and depends on the cancer type and phase [12, 13]. The overexpression of SIRT1 was correlated with metastasis in pancreatic ductal adenocarcinoma [14]. SIRT1 is also overexpressed in hepatocellular carcinoma (HCC), and has been shown to promote tumorigenicity, metastasis, and chemoresistance [15]. These results suggested testing SIRT1 inhibitors against tumor cell-lines. Some of them are shown in figure 1.

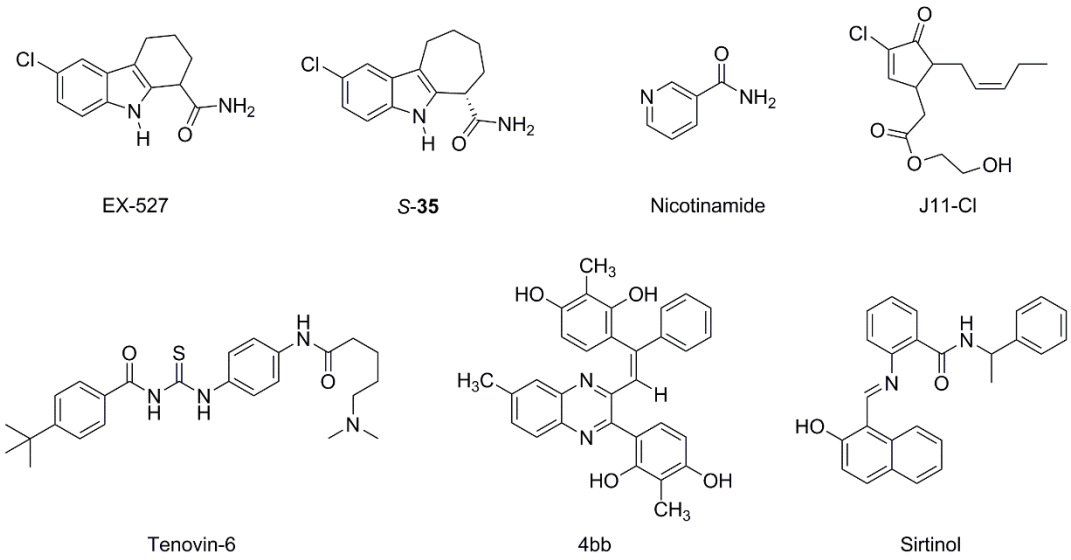

Fig 1. EX-527 and other SIRT1 inhibitors that were tested in various cancer models.

The sirtuin inhibitor nicotinamide has been shown to reduce the proliferation of pancreatic cancer cells, to induce the apoptosis in breast cancer cells, and to enhance their sensibility to cytotoxic agents [16, 17]. The inhibitor 4bb displayed a cytotoxic activity against colon cancer HCT-116 cells, and a mechanism involving p53 as a substrate of SIRT1 was proposed [18]. A prostaglandin derivative, J11-Cl exhibited antiproliferative activity against SKOV cells through activation of apoptotic or autophagic cell death pathways [19]. Sirtinol and cambinol are β-naphthol containing inhibitors of SIRT1. Sirtinol was shown to induce

senescence-like growth arrest in breast cancer MCF-7 and lung cancer H1299 cells. This effect was accompanied by a reduction of the Ras-MAPK pathway activity [20]. Tenovin-6 is another example of sirtuin inhibitor displaying toxicity on mammalian cancer cells, and able to decrease the growth of tumor xenograft in mice [21]. For some compounds like nicotinamide, sirtinol, and tenovin-6, non-specific inhibition and/or dual inhibition of SIRT1 and SIRT2 may explain in part the observed cytotoxic activities. Indeed, SIRT2 is also a potential therapeutic target in several diseases, including cancer [22].

SIRT1 overexpression in several kinds of tumors correlates strongly with attenuated p53 transcription dependent apoptosis upon DNA damage and oxidative stress. p53 can be the target of several covalent modifications including phosphorylation and acetylation, and acetylated p53 is activated and stable. SIRT1 counteracts p53-mediated apoptotic pathways by deacetylating it and decreasing its DNA binding [23]. For example, in HCC cell lines (HepG2 and Huh7), treating by EX-527 caused a decrease of sirtuins activity, a significant increase in the acetyl-p53/p53 ratio, and a decrease in HCC cells survival and migration [24]. Therefore, sirtuins activity blockage could be beneficial to HCC treatment. In this study, the data on p53 acetylation status is consistent with the apoptotic behavior of this tumor suppressor protein [24]. In breast cancer cells MCF-7, EX-527, which is more specific for SIRT1 than SIRT2, induced G_1 phase cell cycle arrest, but no increase in p53 acetylation and cytotoxic effects only at high concentration (> 50 µM). However, sirtinol, which is not specific, induced acetylation of p53 and cytotoxic effect. Because SIRT2 is also able to deacetylate p53, the Authors concluded that inhibition of both SIRT1 and SIRT2 is required to induce p53 acetylation and cell death in breast cancer cells [25]. We note here that the doses of EX-527 employed in different studies and cell lines have to be compared carefully, because at high concentration it inhibits SIRT2. Ohanna et al. found that SIRT1 was overexpressed in several melanoma cell lines [26]. The use of anti SIRT1 siRNA in melanoma cells increased the level of p53 acetylation and induced G_0/G_1 cell cycle arrest. Treatment with EX-527 exhibited similar results, which led to cellular senescence rather than a temporary growth arrest [27].

Treatment of two glioma cell lines (U87MG and LN-299) with EX-527 increased the number of apoptotic cells through the induction of caspase [28]. As p53 is a substrate of SIRT1, the Authors proposed that inhibition of SIRT1 by EX-527 increased the activity of p53 [28]. *In vivo*, EX-527 decreased the tumor growth of xenografted mice with human endometrial and lung cancer cells [29, 30]. EX-527 and one of its analogues (*S*)-**35** were described as selective SIRT1 inhibitors, with IC_{50} values in the range of 100 nM for SIRT1 and 2-20 µM for SIRT2, and no activity against a panel of other HDAC and NAD^+-glycohydrolase [7]. They are mixed-type inhibitors against both NAD^+ and acetylated peptide, therefore the nature of the peptide substrates and the concentrations are expected to have a large influence on the IC_{50} values [7, 31]. A crystal structure of (*S*)-**35** in the active site of SIRT1 has been described (PDB: 4I5I) [32]. It represents a useful tool for the design of new inhibitors of SIRT1.

Based on these results, we now report the design, synthesis and assay of new indole compounds derived from EX-527. Envisioned structural modifications involved the removal of the asymmetric carbon and the introduction of hydrophobic substituents of increasing steric

bulk at positon 3 of the indole. This position was chosen because a suitable small hydrophobic pocket is present in the active site of SIRT1. The new compounds were tested against isolated enzymes SIRT1 and SIRT2, with the objective to identify compounds with better activity and/or selectivity for one of the enzymes. Finally, their cytotoxic activities were determined on a panel of nine cell lines, including cancer cell lines.

2. Results and discussion

2.1. Design and synthesis of new EX-527 indole derivatives

The parent indoles EX-527 and analogue (*S*)-**35** possess an asymmetric carbon. Therefore, they have to be used as racemic mixtures or purified by an additional chiral phase preparative chromatography [7]. We designed new indole derivatives in which the aliphatic cycle is opened, consequently removing the asymmetric carbon (Fig. 2). The primary carboxamide group was kept, because it establishes key hydrogen bond interactions with SIRT1. In our new compounds, hydrophobic substituents of varied steric hindrance were added in position 3 of the indole (R groups, Fig. 2). This was intended to optimize the non-bonding interactions with a small hydrophobic pocket of the enzyme, resulting in potential gains in binding energy. The removal of the cycle induces an increase in conformational flexibility of the substituents in position 2 and 3 of the indole. The carboxamide group may therefore not be positioned correctly for optimum hydrogen bond contact with SIRT1 residues, which may decrease the affinity due to an entropy penalty. However, the presence of the substituents in position 3 of the indole (R ≠ H) should partially block the free rotation of the carboxamide in position 2. Consequently, we expected that our design would limit the entropy penalty and that some of the new indole derivatives would maintain a good binding affinity.

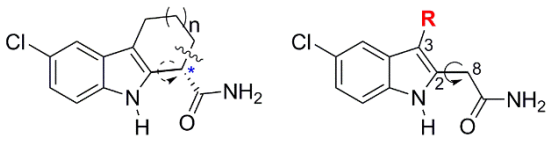

Known inhibitors
of SIRT1/2
n = 1 EX-527
n = 2 (*S*)-**35**

This work
*Removal of the C**
SAR studies on SIRT1/2
R = H, Me, Et, Bn etc.

Fig. 2. Design of new indole derivatives.

The new inhibitors were obtained in three steps (Scheme 1). In the first step, 5-halo-3-alkylindoles that were not commercially available were obtained from 4-halophenylhydrazine and suitable aldehydes via Fischer indole synthesis. The acetate in position 2 was introduced

by the alkylation process developed by Bach's group [33, 34], following an optimized procedure [35]. This method is based on the Pd catalyzed C-H activation of position 2 of the indole *via* an intermediate norbornene adduct. It was found efficient with all 3-alkyl substituted indoles, with the exception of **2i**, bearing a sterically hindered *tert*-butyl group. In the case of 5-chloroindole **1a**, a mixture of mono alkylated **2a** and *bis* alkylated **2a'** was formed. Attempts to introduce a substituted bromoacetate failed, in agreement with previous results [34]. In the third step, the conversion of the ester group into an amide group was performed with anhydrous ammonia in methanol at room temperature, giving the desired products in yields ranging from about 40 to 70%. The structures of the prepared products **3a**-**j** were determined by ^{1}H and ^{13}C NMR. In deuterated DMSO, the NH_2 protons of the amides often appeared as two distinct signals. Little differences in chemical shifts were observed between carbonyl esters (170 ppm) and amides (171 ppm). Final compounds **3a**-**j** were further characterized by HRMS and HPLC.

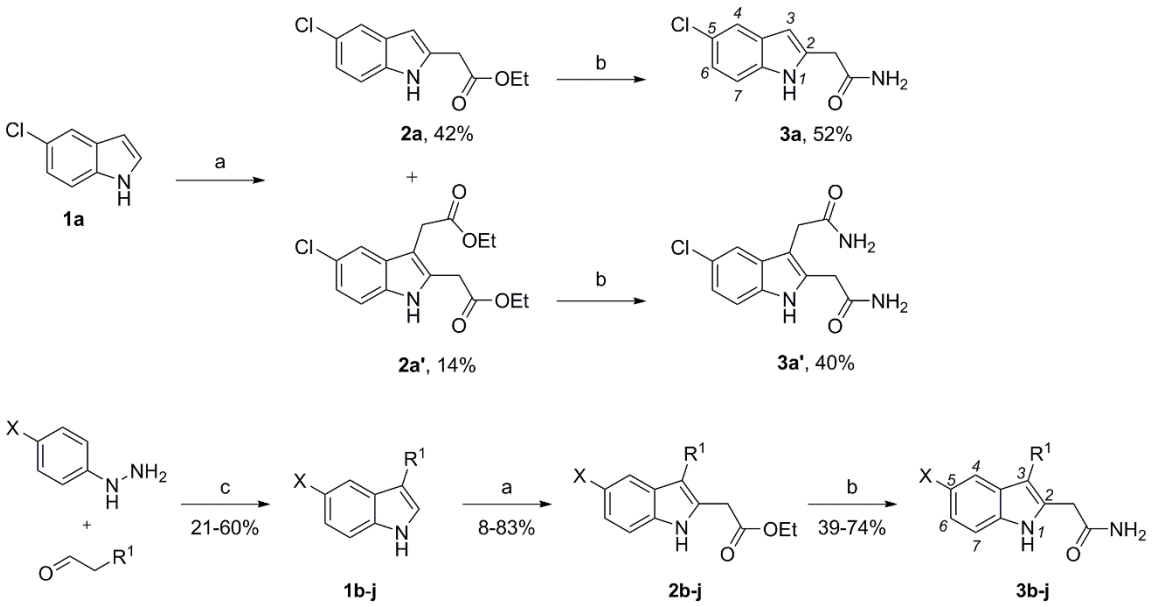

Scheme 1. Synthesis of 2-acetamide indole derivatives **3a**-**j**. Reagents and conditions: (a) $PdCl_2(PhCN)_2$ (10 mol %), norbornene (2 eq.), $NaHCO_3$, ethylbromoacetate, DMF, 1% H_2O, 70°C; (b) NH_3 7M in MeOH, r.t.; (c) AcOH, PhMe, $ZnCl_2$, 120°C.

2.2. Enzymatic assays of the indoles 3a-j on SIRT1 and SIRT2

For the enzymatic assay of SIRT1, we used an acetylated peptide substrate derived from the sequence of p53 RHKK(Ac) with an added tryptophan at the *C*-terminal end. The product of the reaction catalyzed by SIRT1 in the presence of NAD^+ is the corresponding deacetylated

peptide. The integration of the areas of the peaks corresponding to these two peptides in a HPLC chromatogram gives directly the percentage of deacetylation and thus the activity of the enzyme. In the presence of inhibitor, the area measured for the deacetylated peptide decreases. This method is not amenable to high-throughput screening but is very reliable. Indeed, as we already reported, it is not susceptible to potential false positive results that can occur with the more widely employed fluorescence-based assay, and it gives a complete readout of all components in the reaction mixture by HPLC [36]. The same substrate and reaction conditions were chosen for SIRT2 assays (Experimental section).

EX-527 was originally described as a very selective inhibitor of SIRT1 over SIRT2 (IC_{50} = 0.098 nM for SIRT1 and IC_{50} = 19.6 µM for SIRT2) [7], but several subsequent reports indicated that the IC_{50} values and the selectivity were highly dependent on assay conditions, particularly the choice of substrate. For example, Disch et al reported the following values: IC_{50} = 0.26 µM for SIRT1 and 2.9 µM for SIRT2 [37], and Therrien et al.: IC_{50} = 0.5 µM for SIRT1 and 6.5 µM for SIRT2 [38]. Under our assay conditions, the IC_{50} values were 0.69 µM for SIRT1 and 1.5 µM for SIRT2, giving only approximately 2-fold selectivity.

Table 1. Inhibition of SIRT1 and SIRT2 by the indole compounds **3a**-**j**.

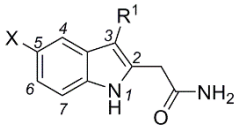

3a-j

Compound	**X**	**R[1]**	**IC_{50} SIRT1 (µM)[a]**	**% inhibition at 10 µM / IC_{50} SIRT2 (µM)[a]**
EX-527	-	-	0.69 [0.53 - 0.90]	84 ± 4 / 1.5 [1.2 - 1.8]
3a	Cl	H	90 [65 - 124]	1.7 ± 5
3a'	Cl	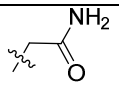	> 100	-14 ± 2
3b	Cl		5.5 [3.8 - 7.9]	0.34 ± 1
3c	Cl		14 [10 - 20]	-5.5 ± 3
3d	Cl	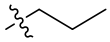	6.8 [4.9 - 9.4]	22 ± 2
3e	Cl	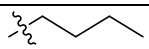	6.0 [4.0 - 8.8]	42 ± 1
3f	Cl	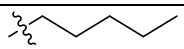	5.5 [3.8 - 7.9]	68 ± 1
3g	Cl	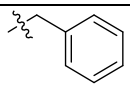	4.9 [3.8 - 6.3]	84 ± 1 / 0.93 [0.62 - 1.4]
3h	Cl		1.6 [1.2 - 2.3]	39 ± 4 (54% at 100 µM)
3i	Cl		7.6 [5.9 - 9.7]	74 ± 1
3j	Br		4.2 [3.2 - 5.3]	38 ± 3

[a]The 95% confidence interval is given in brackets for the IC_{50} values, and the SD is given for the % inhibition. Mean values of at least duplicate experiments.

The IC_{50} values of the new inhibitors were determined and compared to the IC_{50} value of EX-527, which has been tested in the laboratory under the same assay conditions (Table 1). Against SIRT1, none of the tested molecules showed an inhibitory capacity greater than that of EX-527, but indole **3h**, having an isopropyl group at the 3-position, had an IC_{50} only twice as high (1.6 μM versus 0.69 μM for EX-527). Indole **3a**, which is unsubstituted at the 3-position of the indole, was almost inactive (IC_{50} = 90 μM). These results validate the strategy employed here, demonstrating that the opening of the EX-527 cycle (and thus removing the asymmetric carbon) is possible without significant loss of activity, as long as an aliphatic substituent is present in position 3 of the indole to restrain the free rotation of the amide in position 2. The binding mode of compound **3h** is shown in figure 3 and discussed in the docking section (2.4.). IC_{50} values in the same range were obtained for the aliphatic series spanning methyl through pentyl **3b**-**f** (except **3c**, which appeared somewhat less potent) and even for a benzyl substituent in **3g**, indicating that there is some space available for the introduction of bulkier groups without loss of affinity.

In order to evaluate the selectivity of the new compounds for SIRT1 over SIRT2, they were screened at 10 μM against SIRT2 (Table 1). There was a clear correlation between the steric size of the substituents in position 3 of the indole and the inhibitory potency on SIRT2. Small substituents in **3a**-**c** gave no inhibition at 10 μM. The percentage of inhibition then increased steadily from **3d** to **3f** following the increase in chain length, and large substituents in **3g** (benzyl) and **3i** (*tert*-butyl) gave more than 74% inhibition. Because **3h** was the most active compound against SIRT1, we tried to determine its IC_{50} value for SIRT2, but it did not reach full inhibition even at 100 μM, preventing accurate measurement. Therefore, **3h** was more selective for SIRT1 over SIRT2 than EX-527, under our assay procedure. Moreover, the most potent compound **3g** was slightly more active than EX-527 on SIRT2. Indole **3a'** gave a small but reproducible activation of SIRT2 at 10 μM.

To verify that the compound **3h** was not prone to aggregation, which could lead to non-specific inhibition of the enzymes, we carried out a NMR based aggregation assay [39, 40]. An absence of unusual NMR signals upon dilution experiments confirmed the absence of aggregation under the assay conditions (supporting information).

2.3. Cytotoxic activities of the indoles 3a-j

Cytotoxic activities of prepared compounds were tested on nine cell lines, including seven cancer cell lines, the immortalized embryonic kidney 293T cell line, and HUVEC. Results are shown in table 2. Compounds **3a** and **3a'** did not show any activity up to 100 μM, in agreement with their absence of inhibitory activity on isolated SIRT1/2. Compound **3b** was also inactive, indicating that a small methyl substituent in position 3 of the indole was not sufficient to confer a cytotoxic activity. The activity increased with increasing the length of

the alkyl substituent at position 3, from **3c** to **3f**. The most active compounds **3f** and **3g** displayed stronger cytotoxic effects than EX-527 on many of the cell lines tested, and in particular on the colon cancer cell line HT-29. Their IC_{50} values were mostly in the range 20-40 µM. This observation could be correlated with the high inhibitory activity on SIRT2 of these two compounds bearing a bulky substituent in position 3 of the indole. IC_{50} values for the indole **3h** were comparable to those of EX-527 on cancer cell lines. Moreover, **3h** was significantly less cytotoxic than EX-527 on 293T cells and HUVEC.

Table 2. Cytotoxicity of EX-527 derivatives on nine cell lines. IC_{50} values are given in μM ± SD. Camptothecin (CPT) was used as positive control. K562: myelogenous leukemic cells, HCT-116: colon cancer cell line, H460: human large-cell lung carcinoma, HepG2: hepatocellular carcinoma (HCC), A549: adenocarcinomic human alveolar basal epithelial cells, HT-29: colon cancer cell line, MCF-7: breast cancer cell line, 293T: immortalized embryonic kidney cell line, HUVEC: Human Umbilical Vein Endothelial Cells.

Compound	K562	HCT-116	H460	HepG2	A549	HT-29	MCF-7	293T	HUVEC
CPT	0.32±0.13	0.05±0.02	0.12±0.02	0.04±0.01	1.56±0.43	>100	1.67±0.41	5.65±0.62	<0.01
EX-527	60±2	37±1	48±3	44±2	29±3	>100	37±3	51±2	15±2
3a	>100	>100	>100	>100	>100	>100	>100	>100	>100
3a'	>100	>100	>100	>100	>100	>100	>100	>100	>100
3b	>100	>100	>100	>100	>100	>100	>100	>100	>100
3c	87±2	52±3	70±7	>100	>100	>100	>100	77±5	58±3
3d	31±1	32±1	40±2	58±5	35±1	92±4	55±2	43±3	24±3
3e	35±4	31±2	32±1	42±2	30±2	92±3	19±1	53±2	20±3
3f	>100	28±2	30±1	45±1	20±3	27±2	29±3	25±1	10±2
3g	36±3	17±1	34±4	26±2	22±1	35±1	42±1	36±2	28±1
3h	51±1	37±1	>100	40±1	48±2	>100	48±3	>100	45±3
3j	47±1	41±3	66±3	93±5	52±3	>100	64±4	49±5	45±3

2.4. Docking studies of indoles 3a-j with SIRT1

The docking analysis was performed using CDOCKER in the Discovery Studio package [41]. The reference compound EX-527 was first docked in the active site of SIRT1 to check the validity of the docking protocol. Indeed, it adopted an identical position than its analog (*S*)-**35** in the reported crystal structure of the (*S*)-**35** / NAD^+ / SIRT1 complex [32]. Experimental IC_{50} values obtained for the inhibitors were then compared to interaction energies determined by CDOCKER (Supporting information). The correlation was generally qualitatively correct: the strongest inhibitors like **3h** gave the highest interaction energies, whereas the weakest inhibitors like **3a** gave the lowest interaction energies. An exception was diamide **2a'**, which was a very weak inhibitor despite a high interaction energy. It is possible that adverse interactions in the hydrophobic pocket of the enzyme with the hydrophilic amide at position 3 have been underestimated by the docking software. Indole **3g**, bearing the most rigid and bulky substituent of the series, failed to fit in the active site, whereas it actually inhibited SIRT1. This may be because a rigid docking protocol was employed here, not accounting

correctly for the flexibility of the NAD^+ binding loop of SIRT1. This loop may move and create a larger cavity, allowing the accommodation of bulkier substituents.

The binding mode of the most potent indole compound **3h** docked with SIRT1 is depicted in Fig. 3. All the non-covalent interactions between the inhibitor and the active site amino acids of SIRT1 identified in the crystal structure of (*S*)-**35** are also present in the docked structure of **3h**.

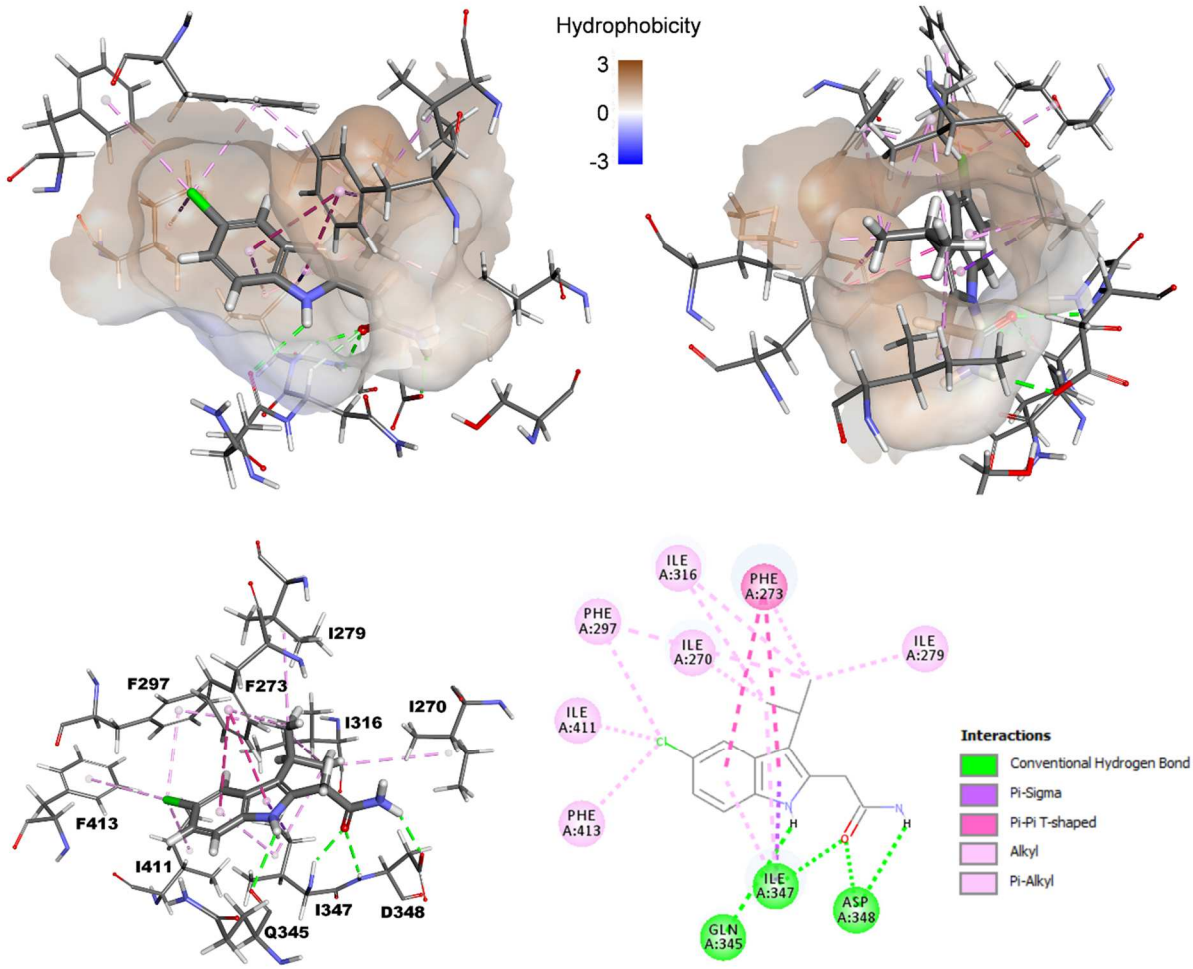

Fig. 3. Indole **3h** docked in the active site of SIRT1 (4I5I). *Top*: Two different views of the amino acids of the active site in interaction with the inhibitor **3h** are drawn (thin lines), and the hydrophobic surface of the enzyme pocket is computed. *Bottom left*: Amino acids of the active site in interaction with **3h** are drawn (thin lines), and the interactions are displayed with dashed lines, color-coded. *Bottom right*: Corresponding 2D map.

2.5. Crystal structure of indole 3j

Key hydrogen bonds involving the carboxamide group of compound (*S*)-**35** were present in its crystal structure with SIRT1 [32]. Hydrogen bonds are directional, and their strength is very sensitive to the alignment of the atoms involved. Therefore, we supposed that the preferred orientation of the carboxamide relative to the indole core in the unbound inhibitors could be important for the affinity. The rotation along the simple bond C2-C8 dictates the orientation of the carboxamide. Our new series of compounds has more potential degrees of freedom along this bond than the parent cyclized compound. To determine the lowest energy conformation in the solid state (which may differ from that in solution), we obtained a crystal structure of compound **3j**. The dihedral angle between atoms N1, C2, C8 and C9 in compound

(*S*)-**35** (Θ) in interaction with SIRT1 was 92.5° (and it was 91.6° in the docked conformation of **3j**). The corresponding angle in the crystal structure of the compound **3j** alone (Θ') was 77.5°. They differed from only 15°, indicating that the most stable conformation of compound **3j** is very similar to the bioactive (SIRT1 bound) conformation of (*S*)-**35** (Fig. 4). It must be noted that the conformation of **3j** with an opposite dihedral angle Θ' = -77.5° was, as expected, equally present in the crystal structure (see the supporting information for additional graphical representations of both conformations). Indeed, both conformations have the same energy because the indole ring is planar.

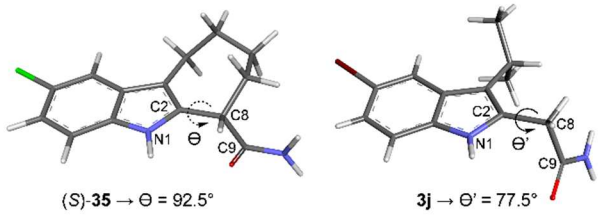

Fig. 4. *Left*: conformation of bound (*S*)-**35** in the crystal structure with SIRT1 (4I5I) [32]. Right: conformation of **3j** in its crystal structure (not bound to SIRT1), CDCC deposition number: 1983558.

3. Conclusion

During the course of this work, a series of indoles designed from EX-527 was prepared in three steps from easily accessible commercial products. Fischer indole synthesis was followed by functionalization at position 2 via palladium catalyzed C-H activation, and amide formation. The prepared products were first tested against SIRT1. Several molecules prepared have inhibitory activities close to that of the reference molecule. This result validates the strategy employed, which makes it possible to remove the asymmetric carbon present in EX-527, and to readily explore the hydrophobic pocket of the active site of SIRT1 with a variety of hydrophobic substituents at the 3-position of the molecule indole. The docking data were generally in agreement with the results of enzymatic inhibitions, which makes it possible to design of new series of inhibitory molecules of SIRT1 by using this method.

The selectivity for SIRT1 was determined by testing the series of inhibitors on SIRT2. Under our assay conditions, compounds **3b**, **3j** and **3h** (our most SIRT1-active compound) appeared to be more selective for SIRT1 over SIRT2 than EX-527. However, the role of SIRT2 as a potential therapeutic target in cancer and other diseases is also the subject of recent studies [22]. Interestingly, compounds bearing bulky substituents in the position 3 of the indole like **3f** and **3g**, displaying significant inhibition of SIRT2 combined with cytotoxic activity, could constitute starting point for further SAR studies on SIRT2 inhibitors.

The next step is the determination of effects of these inhibitors on tumor cell lines, in combination with added cytotoxic agents. Moreover, the expression of biomarkers will provide guidance on the signaling pathways affected by the products. Among the markers that could be studied, the expression and rate of p53 acetylation will be evaluated. The characterization of markers modulated by the effect of the drug candidate is a key element.

Indeed, the presence of this marker in a tumor can guide the therapeutic use in the context of precision medicine. Precision medicine in oncology has led to the arrival of new antitumor agents that may be effective for a limited number of patients. The use of SIRT1 inhibitors could be part of this type of approach.

4. Experimental section

4.1. Chemistry

Melting points were determined on a Stuart SMP3 Instrument and are uncorrected. ^{1}H NMR and ^{13}C NMR spectra were recorded on 400 MHz ^{1}H (100 MHz ^{13}C) BRUKER spectrometer in deuterochloroform (with residual chloroform as an internal reference, calibrated at 7.26 ppm for ^{1}H and 77.00 ppm for ^{13}C) or in deuterated dimethylsulfoxide with dimethylsulfoxide as an internal reference (calibrated at 2.50 ppm for ^{1}H and 40.00 ppm for ^{13}C). Chemical shift values are reported in ppm (δ). Coupling constant values *J* are reported in Hz. HRMS spectra were recorded at the "Institut de Chimie Organique et Analytique" in Orleans, France, on a Q-TOF maXis instrument by ESI in positive mode. Analytical TLC was performed on fluorescent silica gel plates. Visualization was accomplished with UV light. Column flash chromatography was performed using 32-63 µm silica gel. Solvents for extraction and chromatography were reagent grade. Indoles **1a** and **1b** are commercially available. The purity of compounds **3a**-**j** was greater than 96%, as demonstrated by HPLC and ^{1}H NMR.

4.2. HPLC chromatograms

Volumes of 5 µL of 1 mM solutions of compounds dissolved in H_2O with 10% DMSO were injected. Analytical HPLC (Shimadzu Prominence) was carried out using a Phenomenex Luna C18 column (5 µm, 4.6 mm × 250 mm). Solvent A was water with 0.1% TFA, and solvent B was 70% acetonitrile aqueous solution with 0.09% TFA. The products were detected at 220 nm. The indoles **3a**-**j** were separated with a linear gradient from 10 to 100% B in 30 min, at a flow rate of 1 mL/min.

4.3. General procedure for the preparation of 3-alkyl-indoles

Phenylhydrazine hydrochlorides (5 mmol), aldehydes (5 mmol), and AcOH (25 mL) were added in PhMe (250 mL) and the mixture was refluxed for 3 h. PhMe and unreacted aldehyde were then removed by distillation under vacuum. The remaining orange oil was used without purification for the next step. Anhydrous $ZnCl_2$ (2.5 mmol) was added and this mixture was heated 3 h at 100 °C. At the end of the reaction, a black-colored gel was obtained. This gel was extracted by adding water and CH_2Cl_2. The organic layer was washed with water, dried over $MgSO_4$, and concentrated under vacuum. The residue was purified with AcOEt/CycloHex mixture, on a silica gel column chromatography, yielding yellow to brown 3-alkyl-indoles **1c**-**j**.

4.3.1 5-Chloro-3-ethyl-1*H*-indole **1c** [42]

The compound was obtained in 28% yield. ^{1}H NMR (400 MHz, $CDCl_3$) δ_H 1.34 (3H, t, *J* = 7.6 Hz, CH_3), 2.76 (2H, q, *J* = 7.6 Hz, CH_2), 7.01 (1H, s, H2), 7.15 (1H, dd, *J* = 8.6, 2.0 Hz, H6), 7.27 (1H, d, *J* = 8.6 Hz, H7), 7.59 (1H, d, *J* = 2.0 Hz, H4), 7.95 (1H, br s, H1). ^{13}C NMR (100 MHz, $CDCl_3$) δ_C 14.37, 18.20, 112.01, 118.49, 118.64, 121.89, 122.13, 124.81, 128.58, 134.74.

4.3.2. 5-Chloro-3-propyl-1*H*-indole **1d** [43]

The compound was obtained in 21% yield. ^{1}H NMR (400 MHz, $CDCl_3$) δ_H 1.02 (3H, t, *J* = 7.4 Hz, CH_3), 1.74 (2H, sext, *J* = 7.4 Hz, CH_2), 2.71 (2H, t, *J* = 7.4 Hz, CH_2), 7.01 (1H, s, H2), 7.15 (1H, dd, *J* = 8.6, 1.8 Hz, H6), 7.27 (1H, d, *J* = 8.4 Hz, H7), 7.59 (1H, d, *J* = 1.7 Hz, H4), 7.99 (1H, br s, H1). ^{13}C NMR (100 MHz, $CDCl_3$) δ_C 14.12, 23.28, 27.13, 112.01, 116.78, 118.56, 122.05, 122.58, 124.80, 128.81, 134.69.

4.3.3. 3-Butyl-5-chloro-1*H*-indole **1e** [42]
The compound was obtained in 41% yield. ^{1}H NMR (400 MHz, $CDCl_3$) δ_H 0.97 (3H, t, *J* = 7.4 Hz, CH_3), 1.42 (2H, sext, *J* = 7.4 Hz, CH_2), 1.68 (2H, quint, *J* = 7.4 Hz, CH_2), 2.71 (2H, t, *J* = 7.4 Hz, CH_2), 6.99 (1H, s, H2), 7.13 (1H, dd, *J* = 8.6, 1.6 Hz, H6), 7.25 (1H, d, *J* = 9.0 Hz, H7), 7.58 (1H, d, *J* = 1.5 Hz, H4), 7.96 (1H, br s, H1). ^{13}C NMR (100 MHz, $CDCl_3$) δ_C 13.93, 22.58, 24.64, 32.22, 111.96, 116.93, 118.49, 121.99, 122.42, 124.73, 128.74, 134.62.

4.3.4. 5-Chloro-3-pentyl-1*H*-indole **1f** [44]
The compound was obtained in 30% yield. ^{1}H NMR (400 MHz, $CDCl_3$) δ_H 0.92 (3H, t, *J* = 7.0 Hz, CH_3), 1.38 (4H, m, 2 x CH_2), 1.70 (2H, quint, *J* = 7.4 Hz, CH_2), 2.70 (2H, t, *J* = 7.4 Hz, CH_2), 6.99 (1H, s, H2), 7.13 (1H, dd, *J* = 8.5, 1.8 Hz, H6), 7.25 (1H, d, *J* = 8.5 Hz, H7), 7.58 (1H, d, *J* = 1.7 Hz, H4), 7.90 (1H, br s, H1). ^{13}C NMR (100 MHz, $CDCl_3$) δ_C 14.07, 22.52, 24.93, 29.75, 31.76, 111.94, 117.03, 118.52, 122.04, 122.39, 124.77, 128.75, 134.62.

4.3.5. 3-Benzyl-5-chloro-1*H*-indole **1g** [45]
The compound was obtained in 60% yield. ^{1}H NMR (400 MHz, $CDCl_3$) δ_H 4.10 (2H, s, CH_2), 6.96 (1H, s, H2), 7.17 (1H, dd, *J* = 8.6, 1.9 Hz, H6), 7.23-7.35 (6H, m, H_{phenyl} and H7), 7.52 (1H, d, *J* = 1.7 Hz, H4), 8.00 (1H, br s, H1). ^{13}C NMR (100 MHz, $CDCl_3$) δ_C 31.36, 112.04, 115.60, 118.59, 122.32, 123.70, 125.08, 126.02, 128.40 (2C), 128.53, 128.56 (2C), 134.74, 140.66.

4.3.6. 5-Chloro-3-isopropyl-1*H*-indole **1h** [46]
The compound was obtained in 40% yield. ^{1}H NMR (400 MHz, $CDCl_3$) δ_H 1.35 (6H, d, *J* = 7.0 Hz, 2 x CH_3), 3.15 (1H, hept, *J* = 7.0 Hz, CH), 6.98 (1H, s, H2), 7.13 (1H, dd, *J* = 8.6, 1.9 Hz, H6), 7.26 (1H, d, *J* = 8.6 Hz, H7), 7.61 (1H, d, *J* = 1.9 Hz, H4), 7.94 (1H, br s, H1). ^{13}C NMR (100 MHz, $CDCl_3$) δ_C 23.25, 25.36, 112.07, 118.89, 120.69, 122.07, 123.84, 124.72, 127.89, 134.90.

4.3.7. 3-*tert*-Butyl-5-Chloro-1*H*-indole **1i** [47]
The compound was obtained in 54% yield. ^{1}H NMR (400 MHz, $CDCl_3$) δ_H 1.44 (9H, s, 3 x CH_3), 6.96 (1H, s, H2), 7.12 (1H, dd, *J* = 8.6, 1.8 Hz, H6), 7.27 (1H, d, *J* = 8.5 Hz, H7), 7.77 (1H, d, *J* = 1.8 Hz, H4), 7.90 (1H, br s, H1). ^{13}C NMR (100 MHz, $CDCl_3$) δ_C 30.64, 31.46, 112.16, 120.64, 120.65, 121.71, 124.41, 126.63, 126.93, 135.50.

4.3.8. 5-Bromo-3-isopropyl-1*H*-indole **1j** [48]
The compound was obtained in 41% yield. ^{1}H NMR (400 MHz, $CDCl_3$) δ_H 1.34 (6H, d, *J* = 6.9 Hz, 2 x CH_3), 3.15 (1H, hept, *J* = 6.9 Hz, CH), 6.96 (1H, s, H2), 7.22 (1H, d, *J* = 8.5 Hz, H7), 7.26 (1H, dd, *J* = 8.5, 1.8 Hz, H6), 7.77 (1H, d, *J* = 1.8 Hz, H4), 7.93 (1H, br s, H1). ^{13}C NMR (100 MHz, $CDCl_3$) δ_C 23.26, 25.34, 112.31, 112.51, 120.50, 121.98, 123.81, 124.62, 128.58, 135.15.

4.4. General procedure for the preparation of indole acetates
A flask equipped with a magnetic stir bar and a rubber stopper was charged with bis(benzonitrile) dichloropalladium(II) $Pd(PhCN)_2Cl_2$ (0.2 mmol), the indole substrate **1a**-**j** (2 mmol), norbornene (4 mmol), and $NaHCO_3$ (8 mmol). The air was evacuated and the flask backfilled with argon and this process was repeated three times. A mixture of water in DMF (water/DMF 1:100) was added via syringe followed by ethyl bromoacetate (4 mmol). The resulting mixture was stirred at room temperature for 10 min. The reaction was then placed in a preheated oil bath at 70°C for appropriate time, typically 14 to 18 h, and vigorous stirring was applied. The reaction mixture was monitored by TLC. Upon completion, the reaction mixture was cooled to room temperature, diluted with AcOEt, washed with water (twice) and brine (once), dried over $MgSO_4$, and concentrated under vacuum. The

residue was submitted to column chromatography by liquid loading to afford ethyl 2-(1*H*-indol-2-yl) acetates **2a-j** as yellow to brown oils.

4.4.1. Ethyl 2-(5-chloro-1*H*-indol-2-yl)acetate **2a** [49, 50]
The compound was obtained in 42% yield. ^{1}H NMR (400 MHz, $CDCl_3$) δ_H 1.30 (3H, t, *J* = 7.1 Hz, CH_3), 3.82 (2H, s, CH_2CO), 4.22 (2H, q, *J* = 7.1 Hz, OCH_2), 6.29 (1H, s, H3), 7.10 (1H, dd, *J* = 8.6, 2.0 Hz, H6), 7.24 (1H, d, *J* = 8.6 Hz, H7), 7.50 (1H, d, *J* = 2.0 Hz, H4), 8.80 (1H, br s, H1). ^{13}C NMR, DEPT (100 MHz, $CDCl_3$) δ_C 14.15 (CH_3), 33.75 (CH_2), 61.53 (CH_2), 101.46 (CH), 111.78 (CH), 119.51 (CH), 121.97 (CH), 125.43 (C), 129.26 (C), 132.12 (C), 134.63 (C), 170.50 (C=O). ^{13}C NMR (100 MHz, $CDCl_3$) δ_C 14.15, 33.75, 61.53, 101.46, 111.78, 119.51, 121.97, 125.43, 129.26, 132.12, 134.63, 170.50.

4.4.2. Diethyl 2,2'-(5-chloro-1*H*-indole-2,3-diyl)diacetate **2a'**
The compound was obtained in 14% yield. ^{1}H NMR (400 MHz, $CDCl_3$) δ_H 1.24 (3H, t, *J* = 7.1 Hz, CH_3), 1.30 (3H, t, *J* = 7.1 Hz, CH_3), 3.65 (2H, s, CH_2CO), 3.85 (2H, s, CH_2CO), 4.13 (2H, q, *J* = 7.1 Hz, OCH_2), 4.22 (2H, q, *J* = 7.1 Hz, OCH_2), 7.10 (1H, dd, *J* = 8.6, 1.6 Hz, H6), 7.22 (1H, d, *J* = 8.6 Hz, H7), 7.53 (1H, d, *J* = 1.6 Hz, H4), 8.91 (1H, br s, H1).

4.4.3. Ethyl 2-(5-chloro-3-methyl-1*H*-indol-2-yl)acetate **2b** [51]
The compound was obtained in 83% yield. ^{1}H NMR (400 MHz, $CDCl_3$) δ_H 1.30 (3H, t, *J* = 7.1 Hz, CH_3), 2.21 (3H, s, CH_3), 3.76 (2H, s, CH_2CO), 4.21 (2H, q, *J* = 7.1 Hz, OCH_3), 7.09 (1H, dd, *J* = 8.6, 1.9 Hz, H6), 7.21 (1H, d, *J* = 8.6 Hz, H7), 7.45 (1H, d, *J* = 2.0 Hz, H4), 8.61 (1H, br s, H1).

4.4.4. Ethyl 2-(5-chloro-3-ethyl-1*H*-indol-2-yl)acetate **2c**
The compound was obtained in 43% yield. ^{1}H NMR (400 MHz, $CDCl_3$) δ_H 1.21 (3H, t, *J* = 7.6 Hz, CH_3), 1.29 (3H, t, *J* = 7.1 Hz, CH_3), 2.68 (2H, q, *J* = 7.6 Hz, CH_2), 3.76 (2H, s, CH_2CO), 4.21 (2H, q, *J* = 7.1 Hz, OCH_2), 7.09 (1H, dd, *J* = 8.6, 1.9 Hz, H6), 7.22 (1H, d, *J* = 8.6 Hz, H7), 7.50 (1H, d, *J* = 1.8 Hz, H4), 8.60 (1H, br s, H1). ^{13}C NMR (100 MHz, $CDCl_3$) δ_C 14.11, 15.40, 17.16, 31.63, 61.43, 111.69, 115.41, 118.02, 121.78, 124.79, 127.38, 128.90, 134.00, 170.60.

4.4.5. Ethyl 2-(5-chloro-3-propyl-1*H*-indol-2-yl)acetate **2d**
The compound was obtained in 51% yield. ^{1}H NMR (400 MHz, $CDCl_3$) δ_H 0.93 (3H, t, *J* = 7.4 Hz, CH_3), 1.29 (3H, t, *J* = 7.1 Hz, CH_3), 1.63 (2H, sext, *J* = 7.4 Hz, CH_2), 2.63 (2H, t, *J* = 7.5 Hz, CH_2), 3.77 (2H, s, CH_2CO), 4.21 (2H, q, *J* = 7.1 Hz, OCH_2), 7.09 (1H, dd, *J* = 8.6, 1.4 Hz, H6), 7.22 (1H, d, *J* = 8.6 Hz, H7), 7.49 (1H, d, *J* = 1.4 Hz, H4), 8.62 (1H, br s, H1). ^{13}C NMR (100 MHz, $CDCl_3$) δ_C 13.97, 14.12, 23.79, 25.91, 31.70, 61.42, 111.66, 113.69, 118.15, 121.77, 124.80, 127.99, 129.31, 134.01, 170.62.

4.4.6. Ethyl 2-(3-butyl-5-chloro-1*H*-indol-2-yl)acetate **2e**
The compound was obtained in 58% yield. ^{1}H NMR (400 MHz, $CDCl_3$) δ_H 0.93 (3H, t, *J* = 7.4 Hz, CH_3), 1.30 (3H, t, *J* = 7.1 Hz, CH_3), 1.36 (2H, sext, *J* = 7.5 Hz, CH_2), 1.57 (2H, quint, *J* = 7.5 Hz, CH_2), 2.65 (2H, t, *J* = 7.5 Hz, CH_2), 3.76 (2H, s, CH_2CO), 4.21 (2H, q, *J* = 7.1 Hz, OCH_2), 7.09 (1H, dd, *J* = 8.6, 2.0 Hz, H6), 7.22 (1H, d, *J* = 8.6 Hz, H7), 7.48 (1H, d, *J* = 1.9 Hz, H4), 8.61 (1H, br s, H1). ^{13}C NMR (100 MHz, $CDCl_3$) δ_C 13.98, 14.12, 22.60, 23.67, 31.68, 32.90, 61.42, 111.66, 113.92, 118.11, 121.76, 124.78, 127.82, 129.26, 134.00, 170.62.

4.4.7. Ethyl 2-(5-chloro-3-pentyl-1*H*-indol-2-yl)acetate **2f**

The compound was obtained in 80% yield. ^{1}H NMR (400 MHz, $CDCl_3$) δ_H 0.89 (3H, t, *J* = 7.0 Hz, CH_3), 1.30 (3H, t, *J* = 7.1 Hz, CH_3), 1.30-1.35 (4H, m, 2 x CH_2), 1.59 (2H, quint, *J* = 7.3 Hz, CH_2), 2.64 (2H, t, *J* = 7.5 Hz, CH_2), 3.76 (2H, s, CH_2CO), 4.21 (2H, q, *J* = 7.1 Hz, OCH_2), 7.09 (1H, dd, *J* = 8.6, 1.9 Hz, H6), 7.22 (1H, d, *J* = 8.6 Hz, H7), 7.48 (1H, d, *J* = 1.8 Hz, H4), 8.61 (1H, br s, H1). ^{13}C NMR (100 MHz, $CDCl_3$) δ_C 14.05, 14.12, 22.56, 23.90, 30.40, 31.70, 31.72, 61.42, 111.66, 113.95, 118.10, 121.75, 124.77, 127.82, 129.24, 134.00, 170.63.

4.4.8. Ethyl 2-(3-benzyl-5-chloro-1*H*-indol-2-yl)acetate **2g**
The compound was obtained in 47% yield. ^{1}H NMR (400 MHz, $CDCl_3$) δ_H 1.27 (3H, t, *J* = 7.1 Hz, CH_3), 3.77 (2H, s, CH_2CO), 4.05 (2H, s, CH_2), 4.19 (2H, q, *J* = 7.1 Hz, OCH_2), 7.09 (1H, dd, *J* = 8.5, 2.0 Hz, H6), 7.16-7.19 (3H, m, H_{phenyl}), 7.22-7.25 (3H, m, H_{phenyl} + H7), 7.38 (1H, d, *J* = 2.0 Hz, H4), 8.78 (1H, br s, H1). ^{13}C NMR (100 MHz, $CDCl_3$) δ_C 14.07, 29.75, 31.70, 61.47, 111.75, 111.80, 118.22, 122.04, 125.12, 125.97, 128.11 (2C), 128.41 (2C), 128.91, 129.34, 133.99, 140.50, 170.47.

4.4.9. Ethyl 2-(5-chloro-3-isopropyl-1*H*-indol-2-yl)acetate **2h**
The compound was obtained in 51% yield. ^{1}H NMR (400 MHz, $CDCl_3$) δ_H 1.29 (3H, t, *J* = 7.1 Hz, CH_3), 1.39 (6H, d, *J* = 7.1 Hz, 2 x CH_3), 3.11 (1H, hept, *J* = 7.1 Hz, CH), 3.78 (2H, s, CH_2CO), 4.20 (2H, q, *J* = 7.1 Hz, OCH_2), 7.08 (1H, dd, *J* = 8.6, 2.0 Hz, H6), 7.22 (1H, d, *J* = 8.6 Hz, H7), 7.64 (1H, d, *J* = 1.9 Hz, H4), 8.56 (1H, br s, H1). ^{13}C NMR (100 MHz, $CDCl_3$) δ_C 14.12, 22.93 (2C), 25.77, 31.97, 61.43, 111.80, 119.34, 119.39, 121.57, 124.49, 126.51, 127.69, 134.24, 170.60.

4.4.10. Ethyl 2-(3-(*tert*-butyl)-5-chloro-1*H*-indol-2-yl)acetate **2i**
The compound was obtained in 8% yield. ^{1}H NMR (400 MHz, $CDCl_3$) δ_H 1.28 (3H, t, *J* = 7.1 Hz, CH_3), 1.52 (9H, s, 3 x CH_3), 3.99 (2H, s, CH_2CO), 4.20 (2H, q, *J* = 7.1 Hz, OCH_3), 7.07 (1H, dd, *J* = 8.5, 1.6 Hz, H6), 7.19 (1H, d, *J* = 8.5 Hz, H7), 7.80 (1H, d, *J* = 1.3 Hz, H4), 8.63 (1H, br s, H1). ^{13}C NMR (100 MHz, $CDCl_3$) δ_C 14.11, 31.87 (3C), 33.29, 34.00, 61.41, 111.63, 121.11, 121.25, 121.41, 124.23, 126.14, 128.36, 134.15, 170.95.

4.4.11. Ethyl 2-(5-bromo-3-isopropyl-1*H*-indol-2-yl)acetate **2j**
The compound was obtained in 71% yield. ^{1}H NMR (400 MHz, $CDCl_3$) δ_H 1.29 (3H, t, *J* = 7.2 Hz, CH_3), 1.39 (6H, d, *J* = 7.2 Hz, 2 x CH_3), 3.12 (1H, hept, *J* = 7.2 Hz, CH), 3.78 (2H, s, CH_2CO), 4.20 (2H, q, *J* = 7.2 Hz, OCH_2), 7.18 (1H, d, *J* = 8.6 Hz, H7), 7.21 (1H, dd, *J* = 8.6, 1.4 Hz, H6), 7.80 (1H, d, *J* = 1.2 Hz, H4), 8.57 (1H, br s, H1). ^{13}C NMR (100 MHz, $CDCl_3$) δ_C 14.15, 22.98 (2C), 25.79, 31.96, 61.47, 112.13, 112.28, 119.34, 122.40, 124.16, 126.38, 128.41, 134.51, 170.62.

4.5. General procedure for the preparation of indole acetamides

A solution of the indole acetate **2a**-**j** (1.5 mmol) in 7 M NH_3 in MeOH (50 mL) was stirred at 20°C for 1-4 days. The reaction was monitored by TLC until completion. After evaporation of the solvent under vacuum, the crude amides were purified by trituration with ether or by column chromatography using a gradient of AcOEt/Cyclohexane (50:50 to 100% AcOEt) as eluent to afford the indole acetamides **3a-j**.

4.5.1. 2-(5-Chloro-1*H*-indol-2-yl)acetamide **3a**
The compound was obtained in 52% yield. MP 186°C. ^{1}H NMR (400 MHz, d6-DMSO) δ_H 3.56 (2H, s, CH_2CO), 6.22 (1H, s, H3), 7.00 (1H, dd, *J* = 8.5, 2.0 Hz, H6), 7.02 (1H, br s, NH_2), 7.32 (1H, d, *J* = 8.5 Hz, H7), 7.46 (1H, d, *J* = 1.9 Hz, H4), 7.48 (1H, br s, NH_2), 11.12 (1H, br s, H1). ^{13}C NMR (100

MHz, d6-DMSO) δ_C 35.62, 100.28, 112.80, 118.84, 120.60, 123.64, 129.71, 135.07, 136.45, 171.13. HRMS (ESI) $[M + H]^+$, calcd: 209.0476, found: 209.0477.

4.5.2. 2,2'-(5-Chloro-1*H*-indole-2,3-diyl)diacetamide **3a'**
The compound was obtained in 40% yield. ^{1}H NMR (400 MHz, d6-DMSO) δ_H 3.46 (2H, s, CH_2CO), 3.61 (2H, s, CH_2CO), 6.94 (1H, br s, NH_2), 7.02 (1H, dd, *J* = 8.5, 2.1 Hz, H6), 7.05 (1H, br s, NH_2), 7.28 (1H, d, *J* = 8.5 Hz, H7), 7.52 (1H, d, *J* = 2.0 Hz, H4), 7.56 and 7.70 (2H, 2 br s, NH_2), 11.07 (1H, s, H1). ^{13}C NMR (100 MHz, d6-DMSO) δ_C 31.77, 33.99, 107.21, 112.75, 117.85, 121.01, 123.46, 129.45, 133.88, 134.41, 171.56, 173.72. HRMS (ESI) $[M + H]^+$, calcd: 266.0691, found: 266.0688.

4.5.3. 2-(5-Chloro-3-methyl-1*H*-indol-2-yl)acetamide **3b**
The compound was obtained in 48% yield. MP 176°C. ^{1}H NMR (400 MHz, d6-DMSO) δ_H 2.15 (3H, s, CH_3), 3.53 (2H, s, CH_2CO), 6.99 (1H, dd, *J* = 8.5, 2.1 Hz, H6), 7.01 (1H, br s, NH_2), 7.28 (1H, d, *J* = 8.5 Hz, H7), 7.40 (1H, d, *J* = 2.1 Hz, H4), 7.41 (1H, br s, NH_2), 10.94 (1H, s, H1). ^{13}C NMR (100 MHz, d6-DMSO) δ_C 8.66, 33.51, 106.93, 112.62, 117.37, 120.57, 123.13, 130.11, 132.33, 134.22, 171.14. HRMS (ESI) $[M + H]^+$, calcd: 223.0633, found: 223.0631.

4.5.4. 2-(5-Chloro-3-ethyl-1*H*-indol-2-yl)acetamide **3c**
The compound was obtained in 48% yield. MP 189-191°C. ^{1}H NMR (400 MHz, d6-DMSO) δ_H 1.12 (3H, t, *J* = 7.4 Hz, CH_3), 2.64 (2H, q, *J* = 7.3 Hz, CH_2), 3.54 (2H, s, CH_2CO), 6.99 (1H, dd, *J* = 8.5, 1.6 Hz, H6), 7.02 (1H, br s, NH_2), 7.30 (1H, d, *J* = 8.5 Hz, H7), 7.44 (2H, br s, H4 and NH_2), 10.85 (1H, s, H1). ^{13}C NMR (100 MHz, d6-DMSO) δ_C 16.10, 17.08, 33.38, 112.75, 113.75, 117.34, 120.51, 123.13, 129.11, 131.81, 134.33, 171.28. HRMS (ESI) $[M + H]^+$, calcd: 237.0789, found: 237.0788.

4.5.5. 2-(5-Chloro-3-propyl-1*H*-indol-2-yl)acetamide **3d**
The compound was obtained in 71% yield. MP 121-123°C. ^{1}H NMR (400 MHz, d6-DMSO) δ_H 0.88 (3H, t, *J* = 7.4 Hz, CH_3), 1.53 (2H, sext, *J* = 7.4 Hz, CH_2), 2.59 (2H, t, *J* = 7.4 Hz, CH_2), 3.53 (2H, s, CH_2CO), 6.98 (1H, dd, *J* = 8.5, 2.1 Hz, H6), 7.01 (1H, br s, NH_2), 7.29 (1H, d, *J* = 8.5 Hz, H7), 7.42 (1H, d, *J* = 2.1 Hz, H4), 7.44 (1H, br s, NH_2), 10.85 (1H, s, H1). ^{13}C NMR (100 MHz, d6-DMSO) δ_C 14.36, 24.14, 25.80, 33.38, 112.00, 112.73, 117.44, 120.46, 123.12, 129.53, 132.37, 134.32, 171.27. HRMS (ESI) $[M + H]^+$, calcd: 251.0946, found: 251.0941.

4.5.6. 2-(3-Butyl-5-chloro-1*H*-indol-2-yl)acetamide **3e**
The compound was obtained in 56% yield. MP 94-96°C. ^{1}H NMR (400 MHz, d6-DMSO) δ_H 0.89 (3H, t, *J* = 7.4 Hz, CH_3), 1.31 (2H, sext, *J* = 7.4 Hz, CH_2), 1.50 (2H, quint, *J* = 7.5 Hz, CH_2), 2.61 (2H, t, *J* = 7.5 Hz, CH_2), 3.53 (2H, s, CH_2CO), 6.98 (1H, dd, *J* = 8.5, 2.0 Hz, H6), 7.01 (1H, br s, NH_2), 7.29 (1H, d, *J* = 8.5 Hz, H7), 7.41 (1H, d, *J* = 1.9 Hz, H4), 7.43 (1H, br s, NH_2), 10.85 (1H, s, H1). ^{13}C NMR (100 MHz, d6-DMSO) δ_C 14.41, 22.52, 23.55, 33.28, 33.36, 112.19, 112.74, 117.38, 120.45, 123.09, 129.47, 132.22, 134.32, 171.25. HRMS (ESI) $[M + H]^+$, calcd: 265.1102, found: 265.1102.

4.5.7. 2-(5-Chloro-3-pentyl-1*H*-indol-2-yl)acetamide **3f**
The compound was obtained in 74% yield. MP 105-107°C. ^{1}H NMR (400 MHz, d6-DMSO) δ_H 0.85 (3H, t, *J* = 6.8 Hz, CH_3), 1.23-1.33 (4H, m, 2 x CH_2), 1.51 (2H, quint, *J* = 7.2 Hz, CH_2), 2.61 (2H, t, *J* = 7.5 Hz, CH_2), 3.53 (2H, s, CH_2CO), 6.98 (1H, dd, *J* = 8.5, 1.9 Hz, H6), 7.01 (1H, br s, NH_2), 7.29 (1H, d, *J* = 8.5 Hz, H7), 7.41 (1H, d, *J* = 1.8 Hz, H4), 7.43 (1H, br s, NH_2), 10.85 (1H, s, H1). ^{13}C NMR (100 MHz, d6-DMSO) δ_C 14.47, 22.55, 23.77, 30.71, 31.63, 33.36, 112.23, 112.74, 117.37, 120.46, 123.10, 129.47, 132.22, 134.33, 171.25. HRMS (ESI) $[M + H]^+$, calcd: 279.1259, found: 279.1256.

4.5.8. 2-(3-Benzyl-5-chloro-1*H*-indol-2-yl)acetamide **3g**
The compound was obtained in 62% yield. MP 114°C. ^{1}H NMR (400 MHz, d6-DMSO) δ_H 3.64 (2H, s, CH_2CO), 4.00 (2H, s, CH_2), 6.97 (1H, dd, *J* = 8.6, 2.0 Hz, H6), 7.06 (1H, br s, NH_2), 7.11-7.15 (1H, m, H_{phenyl}), 7.22-7.26 (5H, m, 4 x H_{phenyl} and H4), 7.31 (1H, d, *J* = 8.6 Hz, H7), 7.50 (1H, br s, NH_2), 11.00 (1H, s, H1). ^{13}C NMR (100 MHz, d6-DMSO) δ_C 29.83, 33.40, 110.93, 112.84, 117.67, 120.72, 123.22, 126.10, 128.63 (2C), 128.73 (2C), 129.29, 133.02, 134.51, 142.02, 171.19. HRMS (ESI) $[M + H]^+$, calcd: 299.0946, found: 299.0951.

4.5.9. 2-(5-Chloro-3-isopropyl-1*H*-indol-2-yl)acetamide **3h**
The compound was obtained in 48% yield. MP 194°C. ^{1}H NMR (400 MHz, d6-DMSO) δ_H 1.31 (6H, d, *J* = 7.1 Hz, 2 x CH_3), 3.14 (1H, hept, *J* = 7.1 Hz, CH), 3.54 (2H, s, CH_2CO), 6.98 (1H, dd, *J* = 8.6, 1.5 Hz, H6), 6.99 (1H, br s, NH_2), 7.30 (1H, d, *J* = 8.4 Hz, H7), 7.39 (1H, br s, NH_2), 7.54 (1H, d, *J* = 1.4 Hz, H4), 10.84 (1H, s, H1). ^{13}C NMR (100 MHz, d6-DMSO) δ_C 23.39 (2C), 25.44, 33.65, 112.89, 117.66, 118.46, 120.25, 122.82, 127.76, 131.01, 134.56, 171.27. HRMS (ESI) $[M + H]^+$, calcd: 251.0946, found: 251.0945.

4.5.10. 2-(3-(*tert*-Butyl)-5-chloro-1*H*-indol-2-yl)acetamide **3i**
The product was obtained from **2i** (23 mg, 0.078 mmol) with 10 mL of a 7 M solution of NH_3 in methanol in 39% yield (8 mg). MP 145°C. ^{1}H NMR (400 MHz, d6-DMSO) δ_H 1.43 (9H, s, 3 x CH_3), 3.71 (2H, s, CH_2CO), 6.98 (1H, dd, *J* = 8.4, 1.8 Hz, H6), 7.00 (1H, br s, NH_2), 7.27 (1H, br s, NH_2), 7.28 (1H, d, *J* = 8.4 Hz, H7), 7.64 (1H, d, *J* = 1.8 Hz, H4), 10.83 (1H, s, H1). ^{13}C NMR (100 MHz, d6-DMSO) δ_C 32.00 (3C), 33.19, 35.71, 112.66, 119.49, 120.18, 120.23, 122.64, 128.53, 130.46, 134.41, 171.77. HRMS (ESI) $[M + H]^+$, calcd: 265.1102, found: 265.1098.

4.5.11. 2-(5-Bromo-3-isopropyl-1H-indol-2-yl)acetamide **3j**
The compound was obtained in 48% yield. MP 183-185°C. ^{1}H NMR (400 MHz, d6-DMSO) δ_H 1.31 (6H, d, *J* = 7.0 Hz, 2 x CH_3), 3.14 (1H, hept, *J* = 7.0 Hz, CH), 3.54 (2H, s, CH_2CO), 7.00 (1H, br s, NH_2), 7.09 (1H, dd, *J* = 8.5, 1.4 Hz, H6), 7.26 (1H, d, *J* = 8.5 Hz, H7), 7.40 (1H, br s, NH_2), 7.68 (1H, d, *J* = 1.0 Hz, H4), 10.86 (1H, s, H1). ^{13}C NMR (100 MHz, d6-DMSO) δ_C 23.41 (2C), 25.43, 33.63, 110.86, 113.41, 117.58, 121.42, 122.80, 128.52, 130.86, 134.78, 171.27. HRMS (ESI) $[M + H]^+$, calcd: 295.0441, found: 295.0438.

4.6. Enzyme Activity Assays

SIRT1, SIRT2 and EX-527 were purchased from Sigma. Reactions mixtures were prepared in 0.5 mL Eppendorf vials with a final volume of 50 µL. The reaction mixtures contained the assay buffer (from the assay Kit Sigma CS1040, pH 8.0), NAD^+ (2 mM), peptide substrate RHKK(Ac)W-NH_2 (250 µM), and compound inhibitor if required (added from stock solutions 10 times more concentrated). The compounds were prepared as stock solutions with 10% DMSO in water so that the final DMSO concentration was 1% in the reaction mixture. In control experiments without compound, the final DMSO concentration was kept at 1% by addition of a solution of 10% DMSO in water. The reaction was started by addition of SIRT1 (the final concentration was approximately 200 nM, according to the nominal concentration given by the provider) or SIRT2 (the final concentration was approximately 100 nM, according to the nominal concentration given by the provider), without preincubation. The reaction mixture was incubated at 37 °C. The incubation time was chosen so that the conversion was kept between 2% and 8%, typically between 30 min and 2 h for SIRT1, depending on SIRT1 batches, and 20 min for SIRT2 (single batch used). This allowed for accurate measurement by HPLC and

ensured initial velocity conditions. Reactions were stopped by addition of 50 μL of 4% TFA in water, and the resulting mixtures were analyzed by analytical HPLC.
Analytical HPLC (Shimadzu Prominence) was carried out using a Phenomenex Luna C18 column (5 μm, 4.6 mm × 250 mm). Solvent A was water with 0.1% TFA, and solvent B was 70% acetonitrile aqueous solution with 0.09% TFA. The products were detected at 220 nm. The peptide substrate RHKK(Ac)W-NH_2 and deacetylated product RHKKW-NH_2 were separated with a linear gradient from 10 to 50% B in 20 min at a flow rate of 1 mL/min. Peak areas were integrated to calculate the percentage of conversion.

4.7. Cytotoxicity Assays

Using the MTT method, compounds were evaluated against a series of human cancer cell lines including K562, HCT-116, H460, HepG2, A549, HT-29, MCF-7 and normal cell lines 293T, HUVEC. Among them, K562, HCT-116 and MCF-7 cell lines were cultured in RPMI-1640 medium, H460, HepG2 and 293T cell lines were cultured in Dulbecco's modified Eagle's medium, A549, HT-29 and HUVEC cell lines were grown in Ham's F-12 medium. All cell lines were supplemented with 10% (V/V) fetal bovine serum, 2.05 mM glutamine and 1% (V/V) penicillin/streptomycin, and were incubated in a humidified atmosphere of 5% CO_2 at 37 °C.
In 96 well plates, cells were seeded in growth medium at 5×10^4 cells/mL, with aliquots of 100 μL cell suspension into each well. Prior to each cytotoxicity experiment, K562 cells were cultured in suspension for 2 h, and other cells were maintained in medium for them to adhere for 24 h. EX-527 and synthesized compounds (including the positive control CPT) were dissolved in DMSO in serial dilutions to give final concentrations of 0.01, 0.1, 1, 10, 100 μM after addition of 0.5 μL/well. Then, the cells were cultured for 48 h, and 20 μL MTT (5 mg/mL) were added to each well. A volume of 100 μL isopropanol hydrochloride was added, and OD values were read at 570 nm and 630 nm for HCT-116, H460, HepG2, A549, HT-29, MCF-7, 293T and HUVEC, and at 490 nm and 630 nm for K562. The IC_{50} values were calculated from the measured OD values.

4.8. Docking calculations

Docking was performed using CDOCKER with a simulated annealing protocol and the CHARMm forcefield in the Discovery Studio package [41]. The SIRT1 catalytic core of the crystal structure 4I5I [32] was prepared by the software's standard "prepare protein" protocol after removal of the NAD^+ cofactor, the inhibitor and the water molecules. Most search parameters were kept default. For each compound, 100 random conformations were generated by molecular dynamics at a target temperature of 1000 K, and 100 orientations were refined. The simulated annealing protocol for docking had a heating target temperature of 700 K (2000 heating steps) and a cooling target temperature of 300 K (5000 cooling steps). The Momany-Rone method was used to calculate the ligands partial charges. A final energy minimization step was applied to each docking pose with 50 steps of steepest descent algorithm followed by up to 200 steps of conjugate-gradient algorithm using an energy tolerance of 0.001 $kcal.mol^{-1}$. Interaction energies of the best poses of each compound with SIRT1 were determined using the CHARMm forcefield.

4.9. NMR aggregation assay

Following a published procedure, six NMR tubes were prepared by serial dilutions of the compound **3h** (from 200 μM to 6 μM) in a final volume of 500 μL, containing 445 μL assay buffer, 50 μL D_2O and 5 μL DMSO (the final concentration of DMSO was 1%, identical to the enzymatic assay) [39, 40].

^{1}H NMR spectra were recorded on a 600 MHz BRUKER AVANCE spectrometer with suppression of water peak using the esgpph pulse program [52]. All parameters, including the number of scans (2048) and the receiver gain were kept constant for all experiments.

4.10. Crystal structure determination of 3j

The used orange crystal of 0.21× 0.10× 0.03 mm was crystallized by slow evaporation of a solution of of **3j** in methanol. Empirical formula $C_{13}H_{15}BrN_2O$, M = 295.17, T = 100(2) K. Monoclinic system, space group P21/n, Z = 4, a = 7.7652(13) Å, b = 9.969(3) Å, c = 16.313(4) Å, α = 90°, β = 93.249(12)° , γ = 90°, V = 1260.7(5) Å^3, d_{calc} = 1.555 g cm^{-3} , F(000) = 600, μ = 4.324 mm^{-1}, λ(CuKα) = 1.54178 Å. 15387 intensity data were collected with a VENTURE PHOTON100 CMOS Bruker diffractometer (Cu-Kα radiation) controlled by APEX2 software package [53], giving 2220 unique reflections. Data integration and global cell refinement were performed with the program SAINT [54]. Data were corrected for absorption by the multiscan semiempirical method implemented in SADABS [55]. The structure was solved by direct methods using SHELXS-97 [56]. Refinement, based on F^2, was carried out by full matrix least squares with SHELXL-2008 software [57]. All non-hydrogen atoms were refined with anisotropic thermal parameters. The hydrogen atoms were located on a difference Fourier map and placed in their geometrically generated positions and allowed to ride on their parent atoms with an isotropic thermal parameter 20 % higher to that of the atom of attachment. Refinement of 158 parameters on F^2 led to R1(F) = 0.0259 calculated with 2106 observed reflections as I ≥ 2 sigma (I) and wR2(F^2) = 0.0656 considering all the 2220 data. Goodness of fit = 1.267. CCDC deposition number: 1983558. The crystal data collection and refinement parameters are given in the supporting information. CCDC 1983558 contains the supplementary crystallographic data for this paper. These data can be obtained free of charge from the Cambridge Crystallographic Data Centre via http://www.ccdc.cam.ac.uk/Community/Requestastructure.

Abbreviations

SIRT1: Silent Information Regulator 1; SAR, structure-activity relationship; TLC, thin layer chromatography; UV, ultraviolet; HRMS, high-resolution mass spectrometry; HPLC, high-performance liquid chromatography; DCM, dichloromethane; DMSO, dimethyl sulfoxide; MTT, 3-(4,5-dimethylthiazol-2-yl)-2,5-diphenyltetrazolium bromide.

Notes

The authors declare no competing financial interest.

Acknowledgments

This work was supported by the Paris Descartes University, the French CNRS and INSERM. We thank Karim Hammad and Regis Guillot respectively for their help with NMR measurements and X-ray diffraction data collection.

References

[1] J.J. McClure, X. Li and C.J. Chou, Advances and challenges of HDAC inhibitors in cancer therapeutics, Adv. Cancer Res. 138 (2018) 183-211.
[2] H. Jing and H. Lin, Sirtuins in epigenetic regulation, Chem. Rev. 115 (2015) 2350-2375.
[3] Y. Wang, J. He, M. Liao, M. Hu, W. Li, H. Ouyang, X. Wang, T. Ye, Y. Zhang and L. Ouyang, An overview of Sirtuins as potential therapeutic target: Structure, function and modulators, Eur. J. Med. Chem. 161 (2019) 48-77.

[4] H. Dai, D.A. Sinclair, J.L. Ellis and C. Steegborn, Sirtuin activators and inhibitors: Promises, achievements, and challenges, Pharmacol. Ther. 188 (2018) 140–154.
[5] C. O'Callaghan and A. Vassilopoulos, Sirtuins at the crossroads of stemness, aging, and cancer, Ageing Cell. 16 (2017) 1208-1218.
[6] Y. Fujita and T. Yamashita, Sirtuins in neuroendocrine regulation and neurological diseases, Front. Neurosci. 12 (2018) 778.
[7] A.D. Napper, J. Hixon, T. McDonagh, K. Keavey, J.-F. Pons, J. Barker, W.T. Yau, P. Amouzegh, A. Flegg, E. Hamelin, R. Thomas, J., M. Kates, S. Jones, M.A. Navia, J.O. Saunders, P.S. DiStefano and R. Curtis, Discovery of indoles as potent and selective inhibitors of the deacetylase SIRT1, J. Med. Chem. 48 (2005) 8045-8054.
[8] S. Broussy, H. Laaroussi and M. Vidal, Biochemical mechanism and biological effects of the inhibition of silent information regulator 1 (SIRT1) by EX-527 (SEN0014196 or selisistat), J. Enzyme Inhib. Med. Chem. 35 (2020) 1124-1136.
[9] M.R. Smith, A. Syed, T. Lukacsovich, J. Purcell, B.A. Barbaro, S.A. Worthge, S.R. Wei, G. Pollio, L. Magnoni, C. Scali, L. Massai, D. Franceschini, M. Camarri, M. Gianfriddo, E. Diodato, R. Thomas, O. Gokce, S.J. Tabrizi, A. Caricasole, B. Landwehrmeyer, L. Menalled, C. Murphy, S. Ramboz, R. Luthi-Carter, G. Westerberg and J.L. Marsh, A potent and selective Sirtuin 1 inhibitor alleviates pathology in multiple animal and cell models of Huntington's disease, Hum. Mol. Genet. 23 (2014) 2995-3007.
[10] S.D. Süssmuth, S. Haider, G.B. Landwehrmeyer, R. Farmer, C. Frost, G. Tripepi, C.A. Andersen, M. Di Bacco, C. Lamanna, E. Diodato, L. Massai, D. Diamanti, E. Mori, L. Magnoni, J. Dreyhaupt, K. Schiefele, D. Craufurd, C. Saft, M. Rudzinska, D. Ryglewicz, M. Orth, S. Brzozy, A. Baran, G. Pollio, R. Andre, S.J. Tabrizi, B. Darpo and G. Westerberg, An exploratory double-blind, randomized clinical trial with selisistat, a SirT1 inhibitor, in patients with Huntington's disease, Br. J. Clin. Pharmacol. 79 (2015) 465-476.
[11] G. Westerberg, J.A. Chiesa, C.A. Andersen, D. Diamanti, L. Magnoni, G. Pollio, B. Darpo and M. Zhou, Safety, pharmacokinetics, pharmacogenomics and QT concentration–effect modelling of the SirT1 inhibitor selisistat in healthy volunteers, Br. J. Clin. Pharmacol. 73 (2015) 477-491.
[12] D.K. Alves-Fernandes and M.G. Jasiulionis, The role of SIRT1 on DNA damage response and epigenetic alterations in cancer, Int. J. Mol. Sci. 20 (2019) 3153.
[13] V. Carafa, L. Altucci and A. Nebbioso, Dual tumor suppressor and tumor promoter action of sirtuins in determining malignant phenotype, Front. Pharmacol. 10 (2019) 38.
[14] S. Li, H. Hong, H. Lv, G. Wu and Z. Wang, SIRT 1 overexpression is associated with metastasis of pancreatic ductal adenocarcinoma (PDAC) and promotes migration and growth of PDAC cells, Med. Sci. Monit. 22 (2016) 1593-1600.
[15] M. Farcas, A.-A. Gavrea, D. Gulei, C. Ionescu, A. Irimie, C.S. Catana and I. Berindan-Neagoe, SIRT1 in the development and treatment of hepatocellular carcinoma, Front. Nutr. 6 (2019) 148.
[16] J.-G. Zhang, G. Zhao, Q. Qin, B. Wang, L. Liu, Y. Liu, S.-C. Deng, K. Tian and C.-Y. Wang, Nicotinamide prohibits proliferation and enhances chemosensitivity of pancreatic cancer cells through deregulating SIRT1 and Ras/Akt pathways, Pancreatology. 13 (2013) 140-146.
[17] T. Wang, H. Cui, N. Ma and Y. Jiang, Nicotinamide-mediated inhibition of SIRT1 deacetylase is associated with the viability of cancer cells exposed to antitumor agents and apoptosis, Oncol. Lett. 6 (2013) 600-604.
[18] A. Ghosh, A. Sengupta, G.P.K. Seerapu, A. Nakhi, E.V.V.S. Ramarao, N. Bung, G. Bulusu, M. Pal and D. Haldar, A novel SIRT1 inhibitor, 4bb induces apoptosis in HCT116 human colon carcinoma cells partially by activating p53, Biochem. Biophys. Res. Commun. 488 (2017) 562-569.
[19] I.H. Tae, E.Y. Park, P. Dey, J.Y. Son, S.-Y. Lee, J.H. Jung, S. Saloni, M.-H. Kim and H.S. Kim, Novel SIRT1 inhibitor 15-deoxy-$\Delta^{12,14}$-prostaglandin J_2 and its derivatives exhibit anticancer activity through apoptotic or autophagic cell death pathways in SKOV3 cells, Int. J. Oncol. 53 (2018) 2518-2530.
[20] H. Ota, E. Tokunaga, K. Chang, M. Hikasa, K. Iijima, M. Eto, K. Kozaki, M. Akishita, Y. Ouchi and M. Kaneki, Sirt1 inhibitor, Sirtinol, induces senescence-like growth arrest with attenuated Ras–MAPK signaling in human cancer cells, Oncogene. 25 (2006) 176-185.
[21] S. Lain, J.J. Hollick, J. Campbell, O.D. Staples, M. Higgins, M. Aoubala, A. McCarthy, V. Appleyard, K.E. Murray, L. Baker, A. Thompson, J. Mathers, S.J. Holland, M.J.R. Stark, G. Pass, J.

Woods, D.P. Lane and N.J. Westwood, Discovery, in vivo activity, and mechanism of action of a small-molecule p53 activator, Cancer Cell. 13 (2008) 454-463.
[22] Y. Wang, J. Yang, T. Hong, X. Chen and L. Cui, SIRT2: Controversy and multiple roles in disease and physiology, Ageing Res. Rev. 55 (2019) 100961.
[23] G. Botta, L.P. De Santis and R. Saladino, Current advances in the synthesis and antitumoral activity of SIRT1-2 inhibitors by modulation of p53 and pro-apoptotic proteins, Curr. Med. Chem. 19 (2012) 5871-5884.
[24] M.P. Ceballos, G. Decándido, A.D. Quiroga, C.G. Comanzo, V.I. Livore, L. F., F. Lambertucci, L. Chazarreta-Cifre, C. Banchio, M.d.L. Alvarez, A.D. Mottino and M.C. Carrillo, Inhibition of sirtuins 1 and 2 impairs cell survival and migration and modulates the expression of P-glycoprotein and MRP3 in hepatocellular carcinoma cell lines, Toxicol. Lett. 289 (2018) 63-74.
[25] B. Peck, C.-Y. Chen, K.-K. Ho, P. Di Fruscia, S.S. Myatt, R.C. Coombes, M.J. Fuchter, C.-D. Hsiao and E.W.-F. Lam, SIRT inhibitors induce cell death and p53 acetylation through targeting both SIRT1 and SIRT2, Mol. Cancer Ther. 9 (2010) 844-855.
[26] M. Ohanna, C. Bonet, K. Bille, M. Allegra, I. Davidson, P. Bahadoran, J.-P. Lacour, R. Ballotti and C. Bertolotto, SIRT1 promotes proliferation and inhibits the senescence-like phenotype in human melanoma cells, Oncotarget. 5 (2014).
[27] M.J. Wilking, C.K. Singh, M. Nihal, M.A. Ndiaye and N. Ahmad, Sirtuin deacetylases: A new target for melanoma management, Cell Cycle. 13 (2014) 2821-2826.
[28] T. Wang, X. Li and S.-I. Sun, EX527, a Sirt-1 inhibitor, induces apoptosis in glioma via activating the p53 signaling pathway, Anti-Cancer Drug. 31 (2020) 19-26.
[29] R. Asaka, T. Miyamoto, Y. Yamada, H. Ando, D.H. Mvunta, H. Kobara and T. Shiozawa, Sirtuin 1 promotes the growth and cisplatin resistance of endometrial carcinoma cells: a novel therapeutic target, Lab. Investig. 95 (2015) 1363-1373.
[30] G. Chen, B. Zhang, H. Xu, Y. Sun, Y. Shi, Y. Luo, H. Jia and F. Wang, Suppression of Sirt1 sensitizes lung cancer cells to WEE1 inhibitor MK-1775-induced DNA damage and apoptosis, Oncogene, (2017) 1-10.
[31] M. Gertz, F. Fischer, G.T.T. Nguyen, M. Lakshminarasimhan, M. Schutkowski, M. Weyand and C. Steegborn, Ex-527 inhibits Sirtuins by exploiting their unique NAD^+-dependent deacetylation mechanism, Proc. Natl. Acad. Sci. USA, (2013) E2772-E2781.
[32] X. Zhao, D. Allison, B. Condon, F. Zhang, T. Gheyi, A. Zhang, S. Ashok, M. Russell, I. MacEwan, Y. Qian, J.A. Jamison and J.G. Luz, The 2.5 Å crystal structure of the SIRT1 catalytic domain bound to nicotinamide adenine dinucleotide (NAD^+) and an indole (EX527 analogue) reveals a novel mechanism of histone deacetylase inhibition, J. Med. Chem. 56 (2013) 963-969.
[33] L. Jiao and T. Bach, Palladium-catalyzed direct 2-alkylation of indoles by norbornene-mediated regioselective cascade C-H activation, J. Am. Chem. Soc. 133 (2011) 12990-12993.
[34] L. Jiao, E. Herdtweck and T. Bach, Pd(II)-Catalyzed regioselective 2-alkylation of indoles via a norbornene-mediated C-H activation: Mechanism and applications, J. Am. Chem. Soc. 134 (2012) 14563-14572.
[35] Y. Zhang, J. Wang, Y. Nian, H. Sun and H. Liu, Palladium-catalyzed regioselective 2-carbethoxyethylation of 1H-indoles by C-H activation: One-step synthesis of ethyl 2-(1H-indol-2-yl) acetates, Organic Chem. Curr. Res. 3 (2014) 124.
[36] K. Cottet, B. Xu, P. Coric, S. Bouaziz, S. Michel, M. Vidal, M.-C. Lallemand and S. Broussy, Guttiferone A aggregates modulate Silent Information Regulator 1 (SIRT1) activity, J. Med. Chem. 59 (2016) 9560-9566.
[37] J.S. Disch, G. Evindar, C.H. Chiu, C.A. Blum, H. Dai, L. Jin, E. Schuman, K.E. Lind, S.L. Belyanskaya, J. Deng, F. Coppo, L. Aquilani, T.L. Graybill, J.W. Cuozzo, S. Lavu, C. Mao, G.P. Vlasuk and R.B. Perni, Discovery of thieno[3,2-*d*]pyrimidine-6-carboxamides as potent inhibitors of SIRT1, SIRT2, and SIRT3, J. Med. Chem. 56 (2013) 3666-3679.
[38] E. Therrien, G. Larouche, N. Nguyen, J. Rahil, A.-M. Lemieux, Z. Li, M. Fournel, T.P. Yan, A.-J. Landry, S. Lefebvre, J.J. Wang, K. MacBeth, C. Heise, A. Nguyen, J.M. Besterman, R. Déziel and A. Wahhab, Discovery of bicyclic pyrazoles as class III histone deacetylase SIRT1 and SIRT2 inhibitors, Bioorg. Med. Chem. Lett. 25 (2015) 2514-2518.

[39] S.R. LaPlante, R. Carson, J. Gillard, N. Aubry, R. Coulombe, S. Bordeleau, P. Bonneau, M. Little, J. O'Meara and P.L. Beaulieu, Compound aggregation in drug discovery: implementing a practical NMR assay for medicinal chemists, J. Med. Chem. 56 (2013) 5142-5150.
[40] S.R. LaPlante, N. Aubry, G. Bolger, P. Bonneau, R. Carson, R. Coulombe, C. Sturino and P.L. Beaulieu, Monitoring drug self-aggregation and potential for promiscuity in off-target *in vitro* pharmacology screens by a practical NMR strategy, J. Med. Chem. 56 (2013) 7073-7083.
[41] D.S. BIOVIA, *Discovery Studio Client v17*. 2017, San Diego: Dassault Systèmes.
[42] R.P. Karuvalam, K.R. Haridas, A.M. Sajith and A. Muralidharan, A facile access to substituted indoles utilizing palladium catalyzed annulation under microwave enhanced conditions, Tetrahedron Lett. 54 (2013) 5126-5129.
[43] I. Choi, H. Chung, J.W. Park and Y.K. Chung, Active and recyclable catalytic synthesis of indoles by reductive cyclization of 2‐(2-nitroaryl)acetonitriles in the presence of Co–Rh heterobimetallic nanoparticles with atmospheric hydrogen under mild conditions, Org. Lett. 18 (2016) 5508-5511.
[44] S. Buchwald, S. Wagaw and O. Geis, Metal-catalyzed arylations of hydrazines, hydrazones, and related substrates, WO 99/43643, (1999) 1-97.
[45] G. Angelovski, M.D. Keränen, P. Linnepe, S. Grudzielanek and P. Eilbracht, A rapid and reliable assay for regioselectivity using fluorescence spectroscopy, Adv. Synth. Catal. 348 (2006) 1193-1199.
[46] H. Yang, P. Sun, Y. Zhu, H. Yan, L. Lu, D. Liu, G. Rong and J. Mao, Palladium-catalyzed synthesis of indoles via intramolecular Heck reaction Catal. Commun. 38 (2013) 21-25.
[47] A. Kulkarni, P. Quang and B. Török, Microwave-assisted solid-acid-catalyzed Friedel–Crafts alkylation and electrophilic annulation of indoles using alcohols as alkylating agents, Synthesis. 23 (2009) 4010-4014.
[48] H. Haning, M. Woltering, U. Mueller, G. Schmidt, C. Schmeck, V. Voehringer, A. Kretschmer and J. Pernerstorfer, Novel heterocyclic thyromimetics, Bioorg. Med. Chem. Lett. 15 (2005) 1835-1840.
[49] Z. Huang, M. Zhang, S.D. Burton, L.N. Katsakhyan and H. Ji, Targeting the Tcf4 $G^{13}ANDE^{17}$ binding site to selectively disrupt β‐catenin/T-cell factor protein-protein interactions, ACS Chem. Biol. 9 (2014) 193-201.
[50] T.-T. Wang, D. Zhang and W.-W. Liao, Versatile synthesis of functionalized β- and γ-carbolines *via* Pd-catalyzed C–H addition to nitriles/cyclization sequences, Chem. Commun. 54 (2018) 2048-2051.
[51] S. Yamazaki, S. Morikawa, K. Miyazaki, M. Takebayashi, Y. Yamamoto, T. Morimoto, K. Kakiuchi and Y. Mikata, Zinc-catalyzed reactions of ethenetricarboxylates with 2-(trimethylsilylethynyl)anilines leading to bridged quinoline derivatives, Org. Lett. 11 (2009) 2796-2799.
[52] T.-L. Hwang and A.J. Shaka, Water suppression that works. Excitation sculpting using arbitrary waveforms and pulsed field gradients, J. Magn. Reson., Ser. A. 112 (1995) 275-279.
[53] *APEX2. Data Collection Software*, Bruker AXS Inc.: Madison, Wisconsin, USA, 2007.
[54] Bruker *SAINT*, Bruker AXS Inc: Madison, Wisconsin, USA, 2007.
[55] *SADABS.2008/1*, Bruker AXS Inc.: Madison, Wisconsin, USA, 2007.
[56] Sheldrick, G. M. *SHELXS-97, Program for crystal structure solution*, University of Gottingen, Germany, 1997.
[57] Sheldrick, G. M. *SHELXL-2008*, Acta Crystallogr., Sect. A: Found. Crystallogr. 2008, 64 112-122.

Synthesis of indole inhibitors of silent information regulator 1 (SIRT1), and their evaluation as potential cytotoxic agents

H. Laaroussi, Y. Ding, T. Yuou, P. Deschamps, M. Vidal, P. Yu, S. Broussy

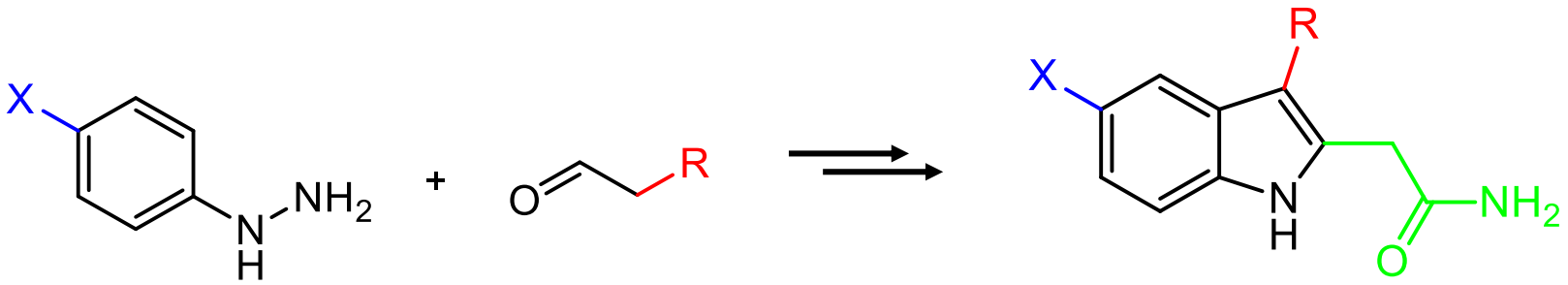

3b-j

X = Cl, Br **R = H, Me, i*Pr*, Bn, …**

3h **X = Cl** **R =**

SIRT1 IC_{50} = 1.6 µM

MCF-7 IC_{50} = 48 µM

3j **X = Br** **R =**

SIRT1 IC_{50} = 4.2 µM

MCF-7 IC_{50} = 64 µM

3h – SIRT1